ChemPubSoc Europe

DOI: 10.1002/chem.201903400

CHEMISTRY A European Journal Full Paper

Synthetic Methods

Synthesis of Thiocyameluric Acid $C_6N_7S_3H_3$, Its Reaction to Alkali Metal Thiocyamelurates and Organic Tris(dithio)cyamelurates

Christian Posern,[a] Carl-Christoph Höhne,[a, b] Uwe Böhme,[a] Claudia Vogt,[a] and Edwin Kroke*[a]

Abstract: Thiocyameluric acid $C_6N_7S_3H_3$, the tri-thio analogue of cyameluric acid, is a key compound for the synthesis of new *s*-heptazine (tri-*s*-triazine) derivatives. Here, two different routes for the synthesis of thiocyameluric acid and its reaction to tris(aryldithio)- and tris(alkyldithio)cyamelurates $C_6N_7(SSR)_3$ are reported as well as transformation to alkali metal thiocyamelurates $M_3[C_6N_7S_3]$, M = Na, K. These compounds were characterised by FTIR, Raman, solution ^{13}C and ^1H NMR spectroscopies, thermal gravimetric analysis (TGA) and elemental analysis. The three (de)protonation steps of thiocyameluric acid were investigated by acid–base titration followed via UV/Vis absorption spectroscopy. While it was not possible to determine the three pK_a values, it could be postulated that the acid strength probably increases in the following order: cyanuric acid ($C_3N_3O_3H_3$) < thiocyanuric acid ($C_3N_3S_3H_3$) < cyameluric acid ($C_6N_7O_3H_3$) < thiocyameluric acid ($C_6N_7S_3H_3$). Single crystals of $Na_3[C_6N_7S_3]\cdot 10\,H_2O$ and $K_3[C_6N_7S_3]\cdot 6\,H_2O$ were obtained and the structures analyzed by single crystal X-ray diffraction. Additionally, quantum chemical calculations were performed to get insights into the electronic structure of thiocyameluric acid and to clarify the thiol–thione tautomerism. Based on a comparison of calculated and measured vibrational spectra it can be concluded that thiocyameluric acid and the di- and mono-protonated anions exist in the thione form.

Introduction

So-called sp^2, 2D or graphitic carbon nitrides "g-C_3N_4", have been extensively investigated in the past decade. (few selected recent reviews: Y. Wang et al.,[1] C. Hu et al.,[2] J. Barrio et al.,[3] F. K. Kessler et al.[4]) In most studies (photo)catalytic properties for highly attractive reactions such as water splitting and CO_2 reduction are reported, which increase with the incorporation of hetero elements (sometimes called doping), including sulfur. It should be pointed out that the so-called sheet-like or layered and in many cases nano-structured "g-C_3N_4" materials are in fact hydrogen-containing *s*-triazine- and/or *s*-heptazine-based oligomers and polymers, which are very easily obtained by thermolysis of melamine $C_3N_3(NH_2)_3$ or melamine precursors such as cyanamide or urea, yielding the molecular intermediates melam $(H_2N)_2C_3N_3\text{-}NH\text{-}C_3N_3(NH_2)_2$ and melem $C_6N_7(NH_2)_3$[5] and at higher temperatures the 1D polymer melon $[C_6N_7(NH_2)(NH)]_n$ and 2D polymers like polyheptazine imide $[C_6N_7(NH)_{1.5}]_n$).[6] Hydrogen-free "g-C_3N_4" have been reported, but are usually not used in the numerous studies on catalytic applications.[7]

Only very few molecular derivatives have directly been obtained from melem, these include triphthalimide $C_6N_7(phthal)_3$,[8] the triphosphinimono derivative $C_6N_7(NPCl_3)_3$, the hydrazine derivative $C_6N_7(NHNH_2)_3$[9] and melemium salts such as $[HC_6N_7(NH_2)_3.]ClO_4\cdot H_2O$.[10] Almost all other derivatives of *s*-heptazine are generated via the formation of cyameluric acid and its potassium salt $K_3[C_6N_7O_3]$.[6]

Cyameluric acid $C_6N_7O_3H_3$ (Scheme 1) and its derivatives belong to the earliest described *s*-heptazine compounds.

[a] C. Posern, C.-C. Höhne, Dr. U. Böhme, C. Vogt, Prof. Dr. E. Kroke
Institut für Anorganische Chemie, TU Bergakademie Freiberg
Leipziger Straße 29, 09599 Freiberg (Germany)
E-mail: kroke@tu-freiberg.de

[b] C.-C. Höhne
Fraunhofer-Institut für Chemische Technologie ICT
76327 Pfinztal (Germany)

Supporting Information and the ORCID identification number(s) for the author(s) of this article can be found under: https://doi.org/10.1002/chem.201903400.

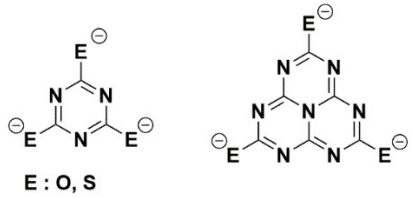

Scheme 1. Principal structures of the *s*-triazine derived cyanurates $[C_3N_3O_3]^{3-}$, and the *s*-heptazine derived cyamelurates $[C_6N_7O_3]^{3-}$ and their thio analogues. For a better comparison with cyameluric acid and cyamelurates we named 2,5,8-trimeracpto-tri-*s*-triazine and its derivatives thiocyameluric acid, thiocyamelurates and the disulfides are named dithiocyamelurates.

Gmelin[11] and Henneberg[12] described cyameluric acid without knowing about its structure. Pauling and Sturdivant[13] suggested the correct tricyclic form in 1937. Cyameluric acid and its salts were characterized by FTIR spectroscopy by Finkel'shtein and Spridonova.[14] In contrast to cyanuric acid $C_3N_3O_3H_3$, which was found to exist in the keto-form, the tautomeric form of cyamluric acid could not be distinguished clearly for a long time and many publications dealt with this question.[15–17] Different crystal structures finally showed that the keto form is favored in the solid state.[15,17] Besides, the crystal structures of cyameluric acid, crystal structures of some alkali metal cyamelurates were reported.[18] Schnick et al. investigated the layer structures of Ca, Zn and Cu cyamelurates crystallized from ammonia solutions.[19]

Cyameluric acid is almost insoluble in most organic solvents and shows a low reactivity. Therefore, the synthesis of organic cyameluric acid esters usually requires cyameluric chloride, which is in turn obtained from potassium cyamelurate as a typical starting material.[20] Triphenylcyamelurate was described by Schroeder and Kober[20] and single crystals could be obtained later by sublimation.[21]

In previous work we described triaryl- and trialkylthiocyamelurates as sulfur analogues.[22,23] While aromatic thiols react easily with cyameluric chloride the nucleophilicity of alkyl thiols is too low for the reaction. Adding a base like *N*,*N*-diisoproylethylamine leads to the desired products. The use of alkali thiolates, which is a typical reaction path for the synthesis of analogous *s*-triazines, leads to decomposition.

So far, cyameluric chloride has been almost unrivaled for the synthesis of new molecular *s*-heptazine derivatives. Very recently, Audebert et al.[24] described 2,5,8-tris(3,5-diethyl-pyrazolyl)-*s*-heptazine. It can be obtained via a two-step synthesis starting from melem. This compound shows, for example towards thiols and amines, a similar reactivity as cyameluric chloride. On the other hand, electrophilic substitutions are not possible. This substance is therefore an interesting approach to obtain new *s*-heptazine derivatives by nucleophilic substitution.

Thiocyameluric acid as the key compound of sulfur substituted *s*-heptazines is not known until now. Contrarily, thiocyanuric acid $C_3N_3S_3H_3$ and its derivatives, especially the trisodium salt, are well known and used industrially. For example, sodium thiocyanurate $C_3N_3S_3Na_3$, which has several trade names and synonyms such as TMT (from trimercapto-*s*-triazine trisodium salt), is used as an effective substance to remove heavy metals from soils or wastewater.[25] In recent reports it was used for electrochemical As^{III} assays,[26] piezoluminescent materials,[27] for hydrogen evolution electrocatalysts,[28] for catalysts for efficient oxygen reduction reactions in fuel cells,[29] for sulfur-rich cathode materials for lithium–sulfur batteries,[30] for corrosion protection of copper,[31] to name only a few examples.

Thiocyanuric acid can be reacted with organo halogenides to give organic thiocyanuric acid esters. The reaction with sulfenyl chlorids leads to dithiocyanurates. These compounds proved to be promising flame retardants for polypropylene.[23,32] The *s*-heptazine derivatives show flame retardant effects, but the high thermal stability is assumed to prevent the release of higher amounts of flame retarding thiyl radical species during the decomposition of polypropylene matrix. The organic dithiocyanurates $C_3N_3(SSR)_3$, show promising effects in contrast to their analogous thiocyanurate derivatives $C_3N_3(SR)_3$. Therefore, higher flame-retardant effects for organic dithiocyamelurates are expected.

Furthermore, sulfur can be used to modify C/N networks. Thiourea[33] and thiocyanuric acid[34] have been used as precursors to synthesize polymeric C_xN_yS photocatalysts, which showed an increased photocatalytic activity compared to the tested "g-C_3N_4". The title compound trimercapto-tri-*s*-triazine alias thiocyameluric acid is a key substance, which would allow access to analogous *s*-heptazine based compounds and materials.

In this paper we report two pathways to synthesize thiocyameluric acid $C_6N_7S_3H_3$ and its further reactions to triphenyl- and triethyl-dithiocyamelurates as well as the crystal structures of the thiocymelurates $Na_3[C_6N_7S_3]\cdot 10\,H_2O$ and $K_3[C_6N_7S_3]\cdot 6\,H_2O$. Theoretical investigations on the electronic structure of thiocyameluric acid and its anion supplement the experimental data.

Results and Discussion

Synthesis of thiocyameluric acid and its dithiocyamelurates

We performed the synthesis of thiocyameluric acid $C_6N_7S_3H_3$ on two different reaction paths (Scheme 2). Path **a**: Cyameluric chloride reacts immediately with H_2S at room temperature in a toluene solution in the presence of *N*,*N*-diisopropylethylamine. No reaction can be observed without the amine base which is already known for the reaction of cyameluric chloride with octylthiol and isopropylthiol.[23] A reaction with sodium sulfide or lithium sulfide does not give the respective thiocyameluric acid salt, either. Path **b**: Triarylthiocyamelurate is cleaved with sodium sulfide. This path is already reported for other heterocyclic compounds.[35] A triarylthiocyamelurate and sodium sulfide are heated under reflux in dimethylformamide. After adding hydrochloric acid to the solution, thiocyameluric

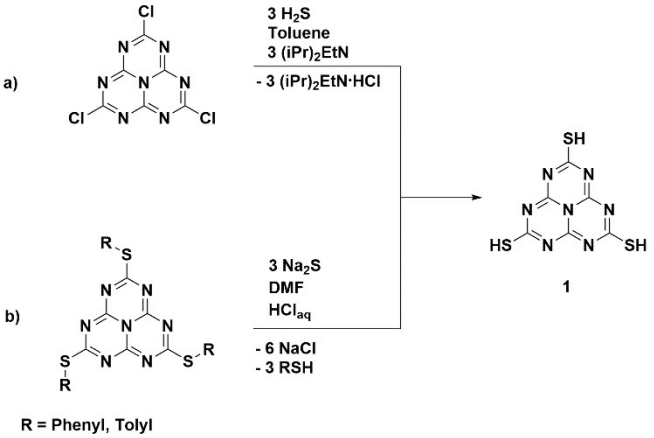

Scheme 2. Two preparative pathways to thiocyameluric acid.

acid (**1**) precipitates as a yellow solid and can be washed with water and dried. However, the sodium salt of **1**, which is the expected intermediate product, cannot be isolated in this way.

From both reaction pathways, path **b** is the appropriate route for the synthesis of larger amounts of **1**. Besides the higher yield of path **b** (40.1 %) over path **a** (28.4 %), the preparation of triarylthiocyamelurates is a well-functioning reaction using unpurified cyameluric chloride as starting material. Path **a** requires cyameluric chloride in high quality. The thiocyameluric acid obtained by path **b** is also easier to purify while the product of path **a** contains impurities after repeated washing with organic solvents and water.

Thiocyameluric acid (**1**) tends to decompose in organic solvents. In different experiments to obtain single crystals the decomposition of **1** was observed and S_8 was isolated. Attempts to increase the yield of the reaction (path **b**) by increasing the reaction time from three to ten hours also were unsuccessful, and complete decomposition was observed. The conversion of the starting material was observed by isolation of the byproducts thiophenol or *p*-thiocresol, respectively. *s*-Heptazine based side products could not be isolated. Attempts to find easier synthetic routes, such as the reaction of cyameluric acid with Lawesson reagent[36] were also not successful.

In this study, triphenyldithiocyamelurate (**2**) and triethyldithiocyamelurate (**3**) were synthesized by the reaction of phenyl sulfenyl chloride or ethyl sulfenyl chloride with thiocyameluric acid (**1**), see Scheme 3. The ratio between **1** and the organic sulfenyl chloride was one-to-two. As already observed by the synthesis of organic dithiocyanurates, threefold substitution is preferred. It is assumed that the increasingly higher solubility of the one-, two- and threefold substituted intermediates are responsible for this reaction behavior. Thiocyameluric acid is nearly not soluble in the reaction medium dichloromethane. Therefore, each thiocyameluric acid molecule, which gains solubility by an organic group, is transported into the reaction medium in which it is surrounded by several organic sulfenyl chlorides. This makes the second and third substitution reaction much faster. By using an excess of the insoluble thiol, side reaction products like organic disulfides are minimized.

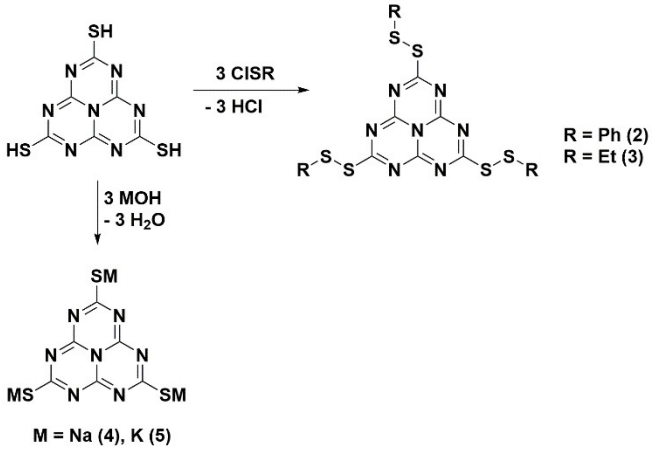

Scheme 3. Synthesis of triphenyldithiocyamelurate (**2**), triethyldithiocyamelurate (**3**), trisodium thiocyamelurate (**4**) and tripotassium thiocyamelurate (**5**).

Spectroscopic characterization

Solution ^{13}C NMR spectroscopy

The compounds **1**, **2**, and **3** were characterized by ^{13}C NMR spectroscopy. The title compound **1** was dissolved and measured in methanol-D_4 (Figure 1).

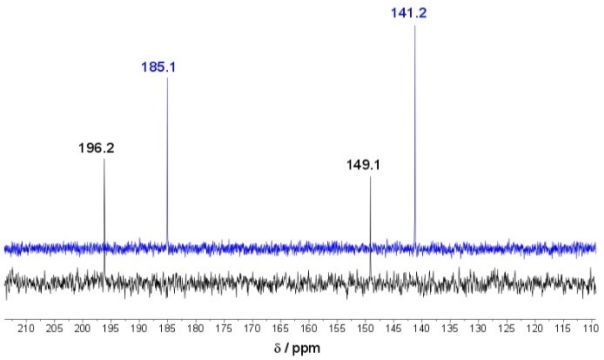

Figure 1. ^{13}C NMR spectra of **1** in methanol-D_4 (blue) and a D_2O/KOH solution of **5** (black).

In a second measurement it was suspended in D_2O and potassium hydroxide was added until a clear solution was obtained (Figure 1). The fully deprotonated anion $[C_6N_7S_3]^{3-}$ corresponding to a solution of the potassium salt **5** is the expected species in this solution.

In the ^{13}C NMR spectra, the typical chemical shifts for the sulfur substituted *s*-heptazine-carbon in **1** (blue curve) is observed at 185.1 ppm and the inner carbon atoms are observed at 141.2 ppm. The signals of the potassium species **5** (black curve) are shifted downfield to 196.2 and 149.1 ppm. In the ^{13}C NMR of compound **2** ($CDCl_3$), the heptazine carbon atoms are detected at 188.3 and 153.0 ppm. In the ^{13}C NMR spectra ($CDCl_3$) the *s*-heptazine carbon signals of compound **3** are observed at 189.9 and 153.6 ppm, respectively. The chemical shift for the *ipso* carbon atoms in **2** and **3** are in the same region as the chemical shifts of triaryl- and trialkylthiocyamelurates.[22]

FTIR and Raman spectroscopy

The FTIR spectra of **1** show the typical *s*-heptazine ring vibrations between 1620 and 1017 cm^{-1}. At 757 cm^{-1} the out of plane vibration of the *s*-heptazine core is observed in the FTIR spectrum. As known from $C_3N_3S_3H_3$[37] the typical C=S vibrations at about 1230 cm^{-1} cannot be observed. N–H vibrations at about 3500 cm^{-1} cannot be observed either.

The Raman spectra of **1** in the thiol- and the thione form were calculated at the M062X/6-311+G(d,p) level of theory and compared to the experimental data (Figure 2). The main difference between the two calculated spectra is the ring breathing vibration which indicates the thione form due to the coupling with the C=S vibration. This vibration is the best indication to differentiate the two tautomeric forms by vibrational spectroscopy. The experimental Raman spectrum shows this ring breathing vibration with a very high intensity at 382 cm^{-1}.

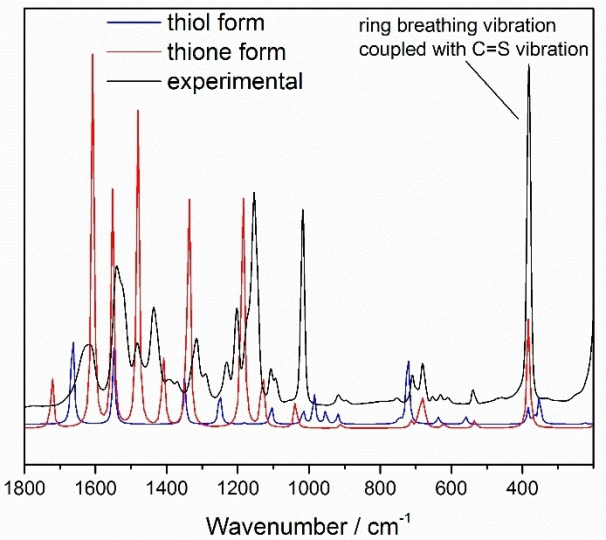

Figure 2. Experimental and calculated RAMAN spectra of **1**.

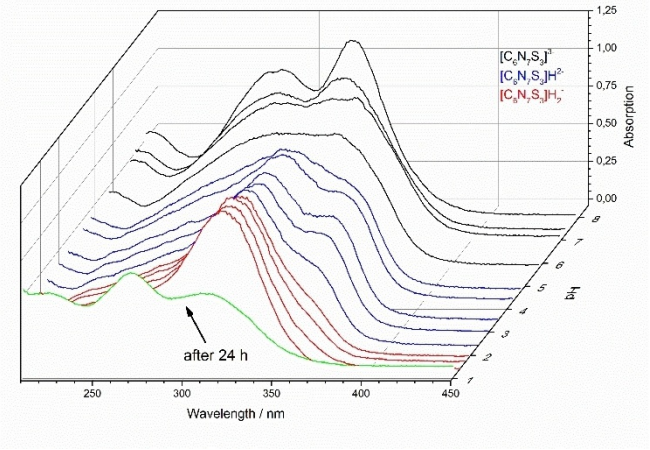

Figure 3. pH-dependent UV/Vis measurements of $Na_3[C_6N_7S_3]$ solutions.

Therefore, we assume that the thione form **1 b** is the preferred tautomeric form of **1** in the solid state (see Scheme 4). The N–H vibrations were not observed, probably because of hydrogen bonds in the solid-state structure.

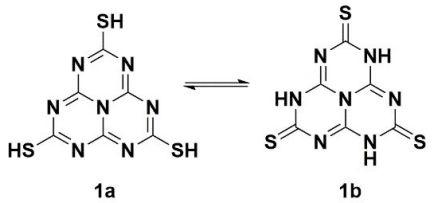

Scheme 4. Thiol–thione tautomerism of thiocyameluric acid (**1**).

The presence of the thione form **1 b** is supported by DFT calculations. The thione form **1 b** was identified as the more stable tautomeric form of **1**. It is 12.7 kJ mol^{-1} lower in Gibbs free energy than the thiol form **1 a**. For further details see Supporting Information.

For the dithiocyamelurates **2** and **3**, the S–S vibration can be observed at 523 cm^{-1} for **2** and at 528 cm^{-1} for **3** in the Raman spectra besides the typical *s*-heptazine vibrations in the ATR, FTIR and Raman spectra.

Acid-base titration and UV/Vis spectra

With UV/Vis spectroscopy different protonated species of the thiocyameluric acid are observable (Figure 3). To an aqueous solution of $Na_3[C_6N_7S_3]$ (6.0×10^{-5} mol L^{-1}) 0.01 M HCl was added stepwise. A UV/Vis-probe head and a pH-probe head were used for the measurement (further information is given in the Supporting Information).

The three pK_a values could neither be differentiated nor determined (see acid–base titration curve in Figure S3). This is most likely due to an overlap of the protonation reactions, which is also indicated by the fact that clear isosbestic points could not be identified in the UV/Vis spectra. Nevertheless, the three different deprotonated species of thiocyameluric acid are detectable during the titration. The fully deprotonated anion $[C_6N_7S_3]^{3-}$ is observed at the start of the measurement at pH 8 (Figure 3). At higher pH values (tested up to pH 12) the same UV/Vis spectra can be observed. The transition steps to the differently protonated species are not sharp. However, all three anionic species can be observed. From a pH value of 7.8 to 4.8, a decrease of the absorption bands of $[C_6N_7S_3]^{3-}$ at 284 and 328 nm is detected (black curves). From pH 4.5 to 2.2 the first protonation step $[C_6N_7S_3]H^{2-}$ is detectable with maxima at 319 and 361 nm. At pH values of 2.1 to 1.0 the twofold protonated species $[C_6N_7S_3]H_2^-$ appears showing an absorption maximum at 324 nm. The fully protonated thiocyameluric acid cannot be observed during the measurement due to the low soluability. After 24 h the UV/Vis measurement of the solution with a pH of 1 was repeated and differences are observed. We assume this observation as a decomposition reaction caused by the protonated sulfur atoms. While the $[C_6N_7S_3]^{3-}$ anion is stable in aqueous solutions, decomposition reactions of the protonated species can be an explanation for the observed decomposition reactions of **1** in solutions. Oxidation reactions to disulfides can be excluded since the observations in degassed solutions are analogous.

The strength of thiocyameluric acid can be estimated by a comparison with cyanuric acid $C_3N_3O_3H_3$, trithiocyanuric acid $C_3N_3S_3H_3$, and cyameluric acid $C_6N_7O_3H_3$. The three corresponding pK_a values decrease and the acid strength increases in the following order: cyanuric acid (6.5, 10.6, $\approx$15)[38] < trithiocyanuric acid (5.71, 8.36 and 11.38)[39] < cyameluric acid (3.0–3.1, 6.1–6.6, 8.4–9.1).[40,41] It is therefore estimated that the acid strength of the title compound is comparable to hydromelonic acid $C_6N_7(NCN)_3H_3$ and the pK_a-values are p$K_{a1}<3$, p$K_{a2}<6$, and p$K_{a3}<8.4$. This is also supported by the relatively low pH values of thiocyameluric salt solutions and the similarity of the acid–base titration curves for hydromelonic acid[40] and thiocyameluric acid (see Figure S3).

Photoluminescence investigations

An aqueous solution of **4** shows a very weak fluorescence at 538 nm (irradiation at 325 nm). For **1** and the two disulfides **2** and **3** we did not observe fluorescence. Other measurements have shown that the substituent on the sulfur atom has a strong influence on the fluorescence.[22,24] Enhanced fluorescence was reported for arylthiocyamelurates dissolved in polypropylene, compared to powder samples of the same *s*-hepatzine compounds.[23]

Thermal behavior of 1 and 2

Thiocyameluric acid **1** was dried at 140 °C under reduced pressure. However, the TGA of **1** (Figure 4) still shows a mass loss of 1.4% up to 140 °C which indicates a high hydrophilicity of **1**. The thermal decomposition takes place in two main decomposition steps at T_{Onset} of 294 and 647 °C. Mass losses of 36.5%

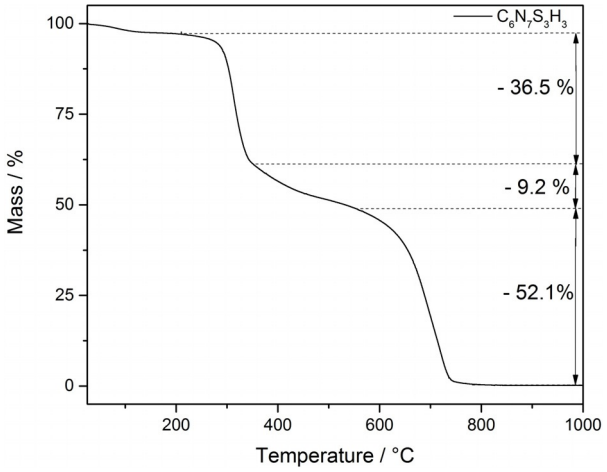

Figure 4. TG of thiocyameluric acid **1** in nitrogen with a heating rate of 10 K min^{-1}.

between 140–350 °C and 52.1% between 475–775 °C are observed. The first step corresponds to the release of three SH species (theoretical mass loss 36.8%). This would mean that after the first decomposition step a carbon nitride network is formed, which consists of *s*-hepatzine units exclusively, that is, $[C_6N_7]_n$, a novel type of polymeric graphitic carbon nitride. Detailed structural investigations are currently performed and will be published in the future.

A weak decomposition step between 350–475 °C is detected with a mass loss of 9.2%. At about 763 °C the residue mass is less than 1.0%. **1** is much more thermally unstable than for example, arylthiocyamlurates like triphenylthiocyamelurate, which starts to thermally decompose under an inert atmosphere at a T_{Onset} of 393 °C. Inter- and intramolecular reactions of **1** involving the acidic H-atoms are assumed as reason for this lower thermal stability.

Triphenyldithiocyamelurate **2** melts at 110–115 °C followed by several decomposition steps above 200 °C (Figure 5). These steps start at a T_{Onset} of 223, 418 and 566 °C, respectively. The

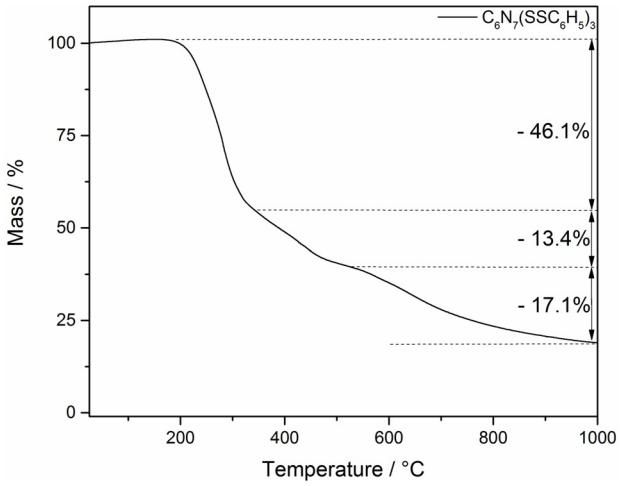

Figure 5. TGA curve of **2** in nitrogen with a heating rate of 10 K min^{-1}.

detected mass loss of 46.1% in the first step releates to the theoretical elimination of two to three phenylthiolate species from **2**. The calculated mass loss for two phenylthiolate species is 36.8% and for three phenylthiolate species 55.2%. The residual mass at 995 °C is 19%.

In contrast to triphenylthiocyamelurate (decomposition T_{Onset} 393 °C[22,23]) the decomposition temperature of **2** is much lower and similar to the analogous *s*-triazine derivative.[16]

The alkyl-substituted disulfide compound **3** shows a similar mulit-step decomposition behavior as **2** (Figure S4). However, the salts **5**·6 H_2O loses the water molecules in separated steps followed by one main decomposition step at around 500 °C (Figure S5).

Crystal structures of $Na_3[C_6N_7S_3]\cdot 10\,H_2O$ and $K_3[C_6N_7S_3]\cdot 6\,H_2O$

All attempts to crystallize **1** were not successful. In the used organic solvents methanol or dimethylsulfoxide **1** is not stable over a longer period of time. However, in aqueous KOH or NaOH solutions no decomposition was observed. Single crystals of $Na_3[C_6N_7S_3]\cdot 10\,H_2O$ and $K_3[C_6N_7S_3]\cdot 6\,H_2O$ are obtained by adding potassium- or sodium hydroxide to an aqueous suspension of **1** followed by slow evaporation in air. Good quality yellow needle-shaped crystals for single crystal X-ray diffraction were obtained. **4**·10 H_2O crystallizes in the monoclinic space group $P2_1/n$, **5**·6 H_2O crystallizes in the monoclinic space group $P2/n$. Figure 6 shows the asymmetric units of both crystal structures.

The bond lengths and angles of the cyameluric core in **4**·10 H_2O and **5**·6 H_2O are in the expected range and comparable to alkali cyamelurates.[18] The C–S bonds in the structures of **4**·10 H_2O (1.7017–1.7123 Å) and **5**·6 H_2O (1.7096–1.7137 Å) are shorter than the C–S bond in the triphenylthiocyamelurate (1.742 Å)[22] but longer than the C=S bond found in thiocyanuric acid $C_3N_3S_3H_3$ in crystal structures containing THF or dioxane (1.640–1.663 Å[42]) which is in its thione form.

Figure 7 shows the coordination sphere of the Na and K atoms in the two crystal structures. The sodium atoms in the structure of **4**·10 H_2O are in distorted octahedral coordination

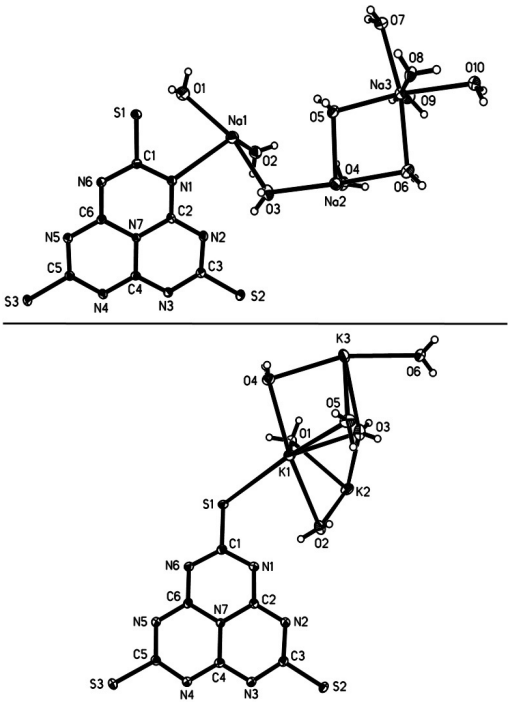

Figure 6. Asymmetric unit of and **4**·10 H_2O (top) and **5**·6 H_2O (bottom). The thermal displacement ellipsoids of all non-hydrogen atoms are drawn at the 50% probability level.

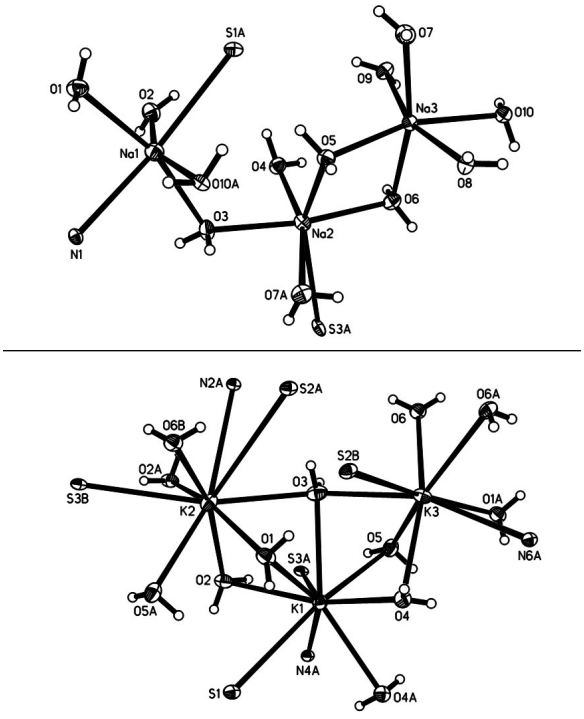

Figure 7. Coordination sphere of the sodium atoms (top) and the potassium atoms (bottom) in the structures of **4**·10 H_2O and **5**·6 H_2O.

geometry. *Na1* is coordinated to four oxygen atoms in equatorial position, one N atom from a *s*-heptazine core, and one S atom from a neighboring thiocyamelurate unit at the apical positions. *Na2 is* coordinated by five oxygen atoms and one S atom. *Na3* is surrounded by six oxygen atoms.

Each potassium atom in the structure of **5**·6 H_2O is higher coordinated and surrounded by eight (K3) or nine (K1 and K2) neighbor atoms. In addition to the oxygen atoms each potassium atoms coordinates sulfur and nitrogen atoms which belong to neighboring heptazine units along all spatial directions. Nitrogen and sulfur atoms from the thiocyamelurate anions act as ligands for the alkali metal cations. The natural charges of both atoms in this anion are very similar (sulfur −0.535, nitrogen −0.597, for details see the Supporting Information). This explains why both atoms are able to act as ligand atoms in these complexes. The coordination of the alkali metal cations generates extended networks, which connect the building blocks of these crystal structures. Furthermore, there are a large number of hydrogen bonds in the solid-state structures of **4**·10 H_2O and **5**·6 H_2O, due to the presence of water in both crystal structures and hydrogen bond acceptors like nitrogen and sulfur.

Besides the intermolecular interactions caused by the Na and K ions, layer-layer distances in the range of π–π-stacking distances are observed in the packings of both structures. In the structure of **4**·10 H_2O these layer-layer distances are 3.353 and 3.488 Å (see Figure 8). The layer-layer distances in **5**·6 H_2O are also in the range of π–π stacks with a length of 3.226 and 3.331 Å. Due to the presence of the central atom *N7*, the heptazine units are usually not stacked exactly on top of each other. To the best of our knowledge, the only exception is the *s*-heptazine based ligand pair (π–π distance: 3.347 Å, N7–N7 distance 3.328 Å) described by Ke et al.[43] The heptazine units of **4**·10 H_2O and **5**·6 H_2O are shifted against each other. This is shown in Figure 8 with the *N7* atoms as reference points. In the structure of **4**·10 H_2O the overlap of the heptazine units is very weak resulting in shifts of 3.313 and 3.797 Å. In the struc-

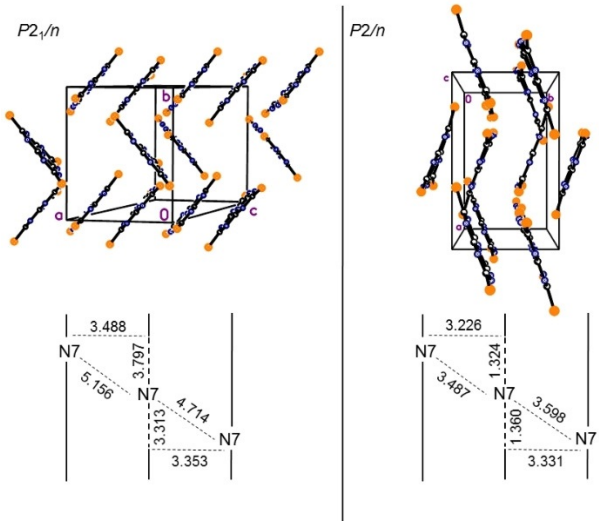

Figure 8. View on the $[C_6N_7S_3]^{3-}$ anions in the structure of **4**·10 H_2O (top left) and **5**·6 H_2O (top right), cations and water excluded. Schematic representation of layer distances [Å] in **4**·10 H_2O (bottom left) and **5**·6 H_2O (bottom right).

ture of **5**·6 H_2O the heptazine units are only shifted by 1.324 and 1.360 Å respectively.

Crystal structures of *s*-triazine derivatives are known for the concept of Piedfort units[44] where for example two stacked trialkoxy-*s*-triazines appear like a hexaalkoxybenzene. Similar stacks are observed in the structure of **5**·6 H_2O (Figure 9). The b-axis passes through the central nitrogen atoms *N7*. Thereby two stacked heptazines can be considered as a Piedfort-like unit, even though they are not stacked in the same way like the triazine derivatives or the *s*-heptazine based Piedfort-pair synthesized by Ke et al.[43] (Additional information about crystal structure data are given in the Supporting Information).

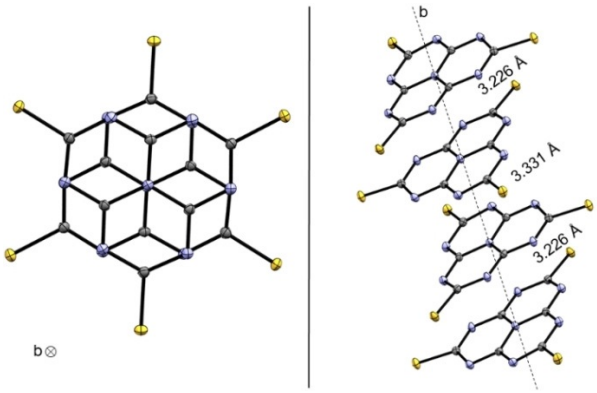

Figure 9. $[C_6N_7S_3]^{3-}$ units in the structure of **5**·6 H_2O with view along the b axis (left) and the course of the b-axis through the *N7* atoms.

Conclusions

In this paper, we present two paths to synthesize thiocyameluric acid **1** and its reaction to triaryl-/trialkyldithiocyamelurates **2** and **3** as well as trialkali metal thiocyamelurates. Compound **4** and **5** were crystallized as water solvates. These compounds open the route to several *s*-hepatzine derivatives, which may be considered for potential applications similar to the analogous *s*-triazine derivatives.

Raman spectroscopy and quantum chemical calculations give information about the tautomeric form of **1** in the solid state, which is in thione form as expected. Additionally, the different protonated species of the thiocyameluric anion were observed by UV/Vis spectroscopy.

The thermal stability of **1** is lower compared to other sulfur compounds of *s*-heptazine, but the dithiocyamelurates **2** and **3** show a promising thermal behavior for the use as flame retardants for selected polymers.

Future studies will focus on the synthesis of larger quantities of **1** and organic dithiocyamelurates to subsequently investigate potential applications as polymer precursors for (catalytically active) C/N- and C/N/S-networks and polymer additives. Of further interest is also the investigation of the reactivity of **1**, for example towards oxidants, silicon and tin chlorides as well as the investigation of the coordination behavior of the title compound and its derivatives towards different types of metal cations.

Experimental Section

General

NMR: Standard ^1H and ^{13}C NMR spectra were recorded on a Bruker Nanobay 400 NMR spectrometer at 293 K [^1H (400 MHz), ^{13}C (101 MHz)]. The chemical shifts are reported relative to tetramethylsilane. **EA**: Elemental analyses were performed with a Vario Micro CHNS analyzer and a CHNS-O analyzer Flash EA 1112 from Thermo Fisher. **FTIR**: FTIR and ATR spectra were recorded at room temperature with a Nicolet 380 FT-IR spectrometer in the range 400–4000 cm^{-1}. **RAMAN**: The Raman spectra were recorded with a BRUKER RFS 100/S spectrometer with a Nd-YAG-laser (max.power 1500 mW, wavelength 1064 nm) and a nitrogen cooled germanium detector. IR and Raman bands were assigned on the basis of quantum chemical optimized molecules. **TGA**: The TGA measurements were performed with a TG 209 F1 Iris ASC from Netzsch in nitrogen with a heating rate of 10 K min^{-1}. **UV/VIS**: The measurement was performed with a JASKO V-650 and a quartz glass probe. **pH-meter**: For the measurement of the pH-values a WTW SenTix81 3 mol KCl electrode and a WTW ionLab pH/ION7320 meter were used. The electrode was calibrated at pH 1, pH 3, pH 6 and pH 9. 0.01 M HCl was added in 100 μL steps from 100 to 1500 μL. Then 0.1 M HCl was added from 1600 to 2000 μL. 1 M HCl was added from 2100 to 4100 μL, then 10 M HCl was added. **Fluorescence**: Fluorescence spectra were recorded with a JASCO FP-850 instrument. The samples were dissolved and placed in $d = 1$ cm cuvettes. **SC-XRD**: Single-crystal X-ray diffraction data sets were collected on a STOE IPDS-2T image plate diffractometer equipped with a low-temperature device with $Mo_{K\alpha}$ radiation ($\lambda = 0.71073$ Å) using ω and ϕ scans. Software for data collection: X-AREA, cell refinement: X-AREA and data reduction: X-RED.[45] The absorption correction was performed with XShape.[46] Structures were solved by direct methods with SHELXS.[47] The structure models were refined by full-matrix least-squares calculations based on F^2 for all reflections using SHELXL.[48] Protons at the water molecules were localized from difference Fourier maps and were freely refined.

Synthesis of thiocyameluric acid

a.) Cyameluric chloride was prepared according the typical procedure[20] and purified via gas phase transport in an Ar-stream at 350 °C. Under Ar-atmosphere 2.0 g (7.2 mmol) cyameluric chloride were dissolved in 100 mL toluene and 4 mL (22.9 mmol) *N*,*N*-diisoporpylethylamine were given to the solution. Under constant stirring H_2S was passed through the solution for one hour. The formation of an orange precipitate was observed immediately. The precipitate was filtered and stirred in dichloromethane, filtered and washed with water. The yellow to orange solid was dried at 120 °C. 550 mg of an orange solid can be obtained (yield: 28.4%). The product still contains impurities (*N*,*N*-diisopropylethylamine hydrochloride).

b.) Tritolylthiocyamelurate was synthezied according to the published route.[22] Sodium sulphide nonahydrate flakes were recrystallized and dried over P_2O_5 under vacuum.[49] 4 g (7.4 mmol) tritolylthiocyamelurate and 5.2 g (67 mmol) sodium sulphide were stirred under reflux in 50 mL dimethylformamide and a few drops of water for three hours. After the mixture was cooled down to room temperature the flask was given into an ice bath and 1 M HCl was added. First, the solution becomes clear and then, after further HCl addition, a pale yellow solid precipitated. The solid is filtered washed with water and cold methanol and dried at 140 °C under vacuum were it changed colour from yellow to orange. 800 mg of an orange solid could be obtained (yield: 40.1%). Anal calc. for

$C_6N_7S_3H_3$ (269.32): calc. C 26.76, N 36.41, H 1.12, S 35.71; found C 25.68, N 36.43, H 1.31, S 33.80 ^{13}C NMR (100.6 MHz, methanol d^4): $\delta = 185.1$ (C–S), 141.2 (CN_2) ppm; ^{13}C NMR (100.6 MHz, D_2O/KOH): $\delta = 196.2$ (C–S), 149.1 (CN_2) ppm; FTIR (KBr): $\tilde{\nu} = 3367$, 2819, 1620, 1379, 1297, 1240, 1190, 1110, 1021, 914, 796, 757, 679, 632 cm^{-1} Raman: $\tilde{\nu} = 2935$, 1617, 1540, 1482, 1436, 1316, 1231, 1203, 1154, 1107, 1017, 918, 754, 709, 681, 653, 630, 539, 382, 195, 109 cm^{-1}.

Synthesis of triphenyldithiocyamelurate (2)

A solution of 153 mg (1.1 mmol) sulfuryl chloride in 1.0 mL dichloromethane and additional 2.0 mL dichloromethane were added to a solution of 125 mg (1.1 mmol) thiophenol in 2.0 mL dichloromethane at room temperature. The solution was protected from light and stirred for 24 h. The obtained red solution and additional 5 mL dichloromethane were added to a dispersion of 150 mg (0.56 mmol) thiocyameluric acid (**1**) in 10.0 mL dichloromethane at room temperature. After 5 days, 25 mL water were added and the emulsion stirred for further 14 days. Afterwards, the dichloromethane phase was separated, extracted three times with alkaline water containing K_2CO_3 and dried with $MgSO_4$. The crude product was purified by column chromatography using a 1:1 mixture of dichloromethane and cyclohexane to remove diphenyl disulfide and afterwards 100% dichloromethane to obtain 75 mg (yield: 34%) of **2** as a yellow powder. Remaining solvent molecules were removed by drying under vacuum at 140 °C. Anal calc. for $C_{24}H_{15}N_7S_6$ (593.81): calc. C 48.5, N 16.5, H 2.5, S 32.4; found C 48.7, N 16.8, H 2.4, S 30.5; ^{1}H NMR (400 MHz, $CDCl_3$): $\delta = 7.25$–7.53 (multiplet) ppm; ^{13}C NMR (100 MHz, $CDCl_3$): $\delta = 188.3$, 153.0 135.0, 130.5–130.2, 129.5–129.4, 129.1–129.1, 127.5, 126.4; ATR-FTIR: $\tilde{\nu} =$ 3055, 1565, 1474, 1439, 1283, 1183, 1076, 1022, 1000, 927, 812, 743, 706, 685 cm^{-1}; Raman: $\tilde{\nu} = 3146$, 3058, 1577, 1491, 1440, 1298, 1222, 1203, 1182, 1160, 1104, 1078, 1045, 1024, 998, 816, 740, 720, 702, 692, 639, 615, 586, 569, 540, 523, 488, 404, 384, 347, 294 cm^{-1}; melting point: 110–115 °C.

Synthesis of triethyldithiocyamelurate (3)

459 mg (3.3 mmol) sulfenyl chloride were added to a solution of 205 mg (3.3 mmol) ethanethiol in 4 mL dichloromethane at room temperature and stirred for 3 h. The obtained yellow solution and additional 10 mL dichloromethane were added to a dispersion of 300 mg (1.1 mmol) thiocyameluric acid (**1**) in 5 mL dichloromethane. After 16 h, 20 mL water were added and the emulsion stirred for additional 22 h. Afterwards, 100 mL dichloromethane and 50 mL water were added. The dichloromethane phase was separated and extracted for three times with water and dried with $MgSO_4$. 450 mg of a yellow powder were obtained after removing the solvent. The crude product was purified by column chromatography using 100% dichloromethane as eluent. 195 mg (yield: 30%) of a yellow powder were obtained after drying under vacuum. Anal calc. for $C_{12}H_{15}N_7S_6$ (449.68): calc. C 32.1, N 21.8, H 3.4, S 42.8; found C 33.7, N 18.5, H 3.5, S 41.1; ^{1}H NMR (400 MHz, $CDCl_3$): $\delta =$ 2.88 (q, $^3J = 7.3$ Hz) ppm, 1.33 (t, $^3J = 7.3$ Hz); ^{13}C NMR (100 MHz, $CDCl_3$): $\delta = 189.9$, 153.6, 32.7, 14.0 ppm; ATR-FTIR: $\tilde{\nu} = 2960$, 2921, 2859, 1578, 1485, 1448, 1372, 1321, 1286, 1189, 1074, 1032, 966, 926, 812, 761 cm^{-1}; Raman: $\tilde{\nu} = 2964$, 2924, 2871, 1592, 1491, 1450, 1417, 1321, 1296, 1273, 1254, 1220, 1101, 1078, 1055, 1034, 969, 814, 764, 717, 637, 576, 528, 379 cm^{-1}; melting point: 153 °C.

Synthesis of trisodiumthiocyamelurate decahydrate (4·10 H_2O)

Sodium hydroxide was added in small portions to an aqueous suspension of **1**. The addition was stopped just before **1** was fully dissolved. The obtained suspension was filtered and evaporated slowly in air. Yellow crystals were obtained. FTIR (KBr): $\tilde{\nu} = 3384$, 1584, 1453, 1411, 1303, 1204, 1088, 1000, 935, 865, 795, 521 cm^{-1}.

Synthesis of tripotassiumthiocyamelurate hexahydrate (5·6 H_2O)

Potassium hydroxide was added in small portions to an aqueous suspension of **1** until a saturated solution is obtained. The solution was filtered and evaporated in the air. Yellow needle-shaped crystals were obtained. FTIR (KBr): $\tilde{\nu} = 3374$, 2497, 2175 1578, 1411, 1292, 1195, 1081, 928, 799, 655, 579, 502 cm^{-1}.

Crystal structure determination

Table 1. Crystallographic and structure refinement data for **4**·10 H_2O and **5**·6 H_2O

	4·10 H_2O	**5**·6 H_2O
chemical formula	$C_6H_{20}Na_3N_7O_{10}S_3$	$C_6H_{12}K_3N_7O_6S_3$
formula mass	515.44	491.71
crystal system	monoclinic	monoclinic
space group	$P2_1/n$	$P2/n$
a [Å]	9.0808(4)	11.7095(4)
b [Å]	11.2072(3)	7.08370(10)
c [Å]	20.2119(9)	20.8523(7)
α [°]	90	90
β [°]	100.419(3)	90.594(3)
γ [°]	90	90
V [Å^3]	2023.06(14)	1729.53(9)
Crystal size [mm]	0.450·0.300·0.250	0.450·0.450·0.120
Z	4	4
F(000)	1064	1000
D_{calcd} [mg m-^{3}]	1.692	1.888
μ ($Mo_{K\alpha}$) [mm^{-1}]	0.492	1.192
Data collection temperature [K]	153	153
Θ range [°]	2.049–27.997	1.986–27.499
h, k, l range	−11/11, −14/14, −26/26	−15/15, −9/9, −27/27
Reflections collected/unique	18913/4868	31915/3977
R_{int}	0.0178	0.0239
Data/restraints/parameters	4868/0/343	3977/0/275
R1, wR2 [$I \geq 2\ \sigma(I)$]	0.0250, 0.0632	0.0266, 0.0698
$R1(F)$[a]/$wR2(F^2)$ (all data)[b]	0.0280, 0.0660	0.0280, 0.0710
S (goodness of fit on F^2)[c]	1.126	1.231
Final $\Delta\rho_{max}/_{min}$ [e Å^{-3}]	0.347/−0.256	0.322/−0.327
CCDC number	1938654	1938655

[a] $R1 = \Sigma\,|F_0| - |F_c|\,/\Sigma\,|F_0|$. [b] $wR2 = [\Sigma w(F_0^2 - F_c^2)^2/\Sigma w(F_0^2)^2]^{1/2}$, $w(F_0^2) + (xP)^2 + yP]^{-1}$ in which $P = [\mathrm{Max}(F_0^2, 0) + 2F_c^2]/3$. [c] $\mathrm{GoF} = (F_0^2 - F_c^2)^2/(n_{obs} - n_{param})]^{1/2}$.

Quantum chemical calculations

The quantum chemical calculations have been performed with GAUSSIAN 16.[50] The molecules have been optimized with M062X/6-311 + G(d,p).[51] The calculation of Hessian-matrices verified the

presence of local minima on the potential energy surface with zero imaginary frequencies. The calculated frequencies have been used to identify the vibrations of the experimental IR- and Raman-spectra. The NBO analysis has been performed with NBO 6.0.[52] Numerical data are listed in the Supporting Information.

Acknowledgements

The authors gratefully acknowledge help from B. Kutzner (NMR), R. Moßig (RAMAN and TG) and C. Hübler (Fluorescence). The authors thank the Computing Centre of the TU Bergakademie Freiberg for computing time at the high-performance computing (HPC) cluster. The authors would like to gratefully thank their colleges from Fraunhofer ICT, Pfinztal: B. Tübke, Y. Galus, I. Kupsch, J. Limburger, W. Schweikert, S. Müller, M. Dörich and C. Fisher for analytical support. Financial support was provided by Fraunhofer ICT and TU Bergakademie Freiberg. The German Research Foundation (DFG) is acknowledged for financial support.

Conflict of interest

The authors declare no conflict of interest.

Keywords: cyameluric acid · heterocycles · sulfur · thermal behavior · triazines

[1] Y. Wang, J. Mao, X. Meng, L. Yu, D. Deng, X. Bao, *Chem. Rev.* **2019**, *119*, 1806.
[2] C. Hu, Y.-R. Lin, H.-C. Yang, *ChemSusChem* **2019**, *12*, 1769.
[3] J. Barrio, M. Shalom, *ChemCatChem* **2018**, *10*, 5573.
[4] F. K. Kessler, Y. Zheng, D. Schwarz, C. Merschjann, W. Schnick, X. Wang, M. J. Bojdys, *Nat. Rev. Mater.* **2017**, *2*, 17030.
[5] F. K. Kessler, A. M. Burow, G. Savasci, T. Rosenthal, P. Schultz, E. Wirnhier, O. Oeckler, C. Ochsenfeld, W. Schnick, *Chem. Eur. J.* **2019**, *25*, 8415.
[6] A. Schwarzer, T. Saplinova, E. Kroke, *Coord. Chem. Rev.* **2013**, *257*, 2032.
[7] a) E. G. Gillan, *Chem. Mater.* **2000**, *12*, 3906; b) J. R. Holst, E. G. Gillan, *J. Am. Chem. Soc.* **2008**, *130*, 7373; c) G. Algara-Siller, N. Severin, S. Y. Chong, T. Björkman, R. G. Palgrave, A. Laybourn, M. Antonietti, Y. Z. Khimyak, A. V. Krasheninnikov, J. P. Rabe, U. Kaiser, A. I. Cooper, A. Thomas, M. J. Bojdys, *Angew. Chem. Int. Ed.* **2014**, *53*, 7450; *Angew. Chem.* **2014**, *126*, 7580.
[8] A. Schwarzer, U. Böhme, E. Kroke, *Chem. Eur. J.* **2012**, *18*, 12052.
[9] T. Saplinova, V. Bakumov, T. Gmeiner, J. Wagler, M. Schwarz, E. Kroke, *Z. Anorg. Allg. Chem.* **2009**, *635*, 2480.
[10] A. Sattler, L. Seyfarth, J. Senker, W. Schnick, *Z. Anorg. Allg. Chem.* **2005**, *631*, 2545.
[11] L. Gmelin, *Ann. Pharm.* **1835**, *15*, 252.
[12] W. Henneberg, *Ann. Chem. Pharm.* **1850**, *73*, 228.
[13] L. Pauling, J. H. Sturdivant, *Proc. Natl. Acad. Sci. USA* **1937**, *23*, 615.
[14] A. I. Finkel'shtein, N. V. Spiridonova, *Russ. Chem. Rev.* **1964**, *33*, 400.
[15] A. Sattler, W. Schnick, *Z. Anorg. Allg. Chem.* **2006**, *632*, 1518.
[16] a) N. E. A. El-Gamel, L. Seyfarth, J. Wagler, H. Ehrenberg, M. Schwarz, J. Senker, E. Kroke, *Chem. Eur. J.* **2007**, *13*, 1158; b) L. Seyfarth, J. Sehnert, N. E. A. El-Gamel, W. Milius, E. Kroke, J. Breu, J. Senker, *J. Mol. Struct.* **2008**, *889*, 217; c) X. Liang, W. Zheng, N.-B. Wong, Y. Shu, A. Tian, *THEOCHEM* **2005**, *732*, 127.
[17] J. Wagler, N. E. A. El-Gamel, E. Kroke, *Z. Naturforsch. B* **2006**, *61*, 975.
[18] E. Horvath-Bordon, E. Kroke, I. Svoboda, H. Fuess, R. Riedel, S. Neeraj, A. K. Cheetham, *Dalton Trans.* **2004**, 3900.
[19] A. Sattler, M. R. Budde, W. Schnick, *Z. Anorg. Allg. Chem.* **2009**, *635*, 1933.
[20] H. Schroeder, E. Kober, *J. Org. Chem.* **1962**, *27*, 4262.
[21] M. R. Schwarz, H. Ehrenberg, M. A. Kloc, E. Kroke, *Heterocycles* **2006**, *68*, 2499.
[22] C. Posern, U. Böhme, J. Wagler, C.-C. Höhne, E. Kroke, *Chem. Eur. J.* **2017**, *23*, 12510.
[23] C.-C. Höhne, C. Posern, U. Böhme, F. Eichler, E. Kroke, *Polym. Degrad. Stab.* **2019**, *166*, 17.
[24] L. Galmiche, C. Allain, T. Le, R. Guillot, P. Audebert, *Chem. Sci.* **2019**, *10*, 5513.
[25] a) N. Meunier, J. F. Blais, M. Lounès, R. D. Tyagi, J. L. Sasseville, *Water Sci. Technol.* **2002**, *46*, 33; b) G. Andreottola, M. Cadonna, P. Foladori, G. Gatti, F. Lorenzi, P. Nardelli, *Water Sci. Technol.* **2007**, *56*, 111; c) Y. Nakamura, A. Umehara, JP 53076992, **1978**.
[26] Y.-H. Yuan, X.-H. Zhu, S.-H. Wen, R.-P. Liang, L. Zhang, J.-D. Qiu, *J. Electroanal. Chem.* **2018**, *814*, 97.
[27] Q. Li, S. Li, K. Wang, Y. Zhou, Z. Quan, Y. Meng, Y. Ma, B. Zou, *J. Phys. Chem. C* **2017**, *121*, 1870.
[28] R. S. Vishwanath, K. Sakthivel, *J. Mater. Chem. A* **2017**, *5*, 2052.
[29] Z. K. Yang, L. Lin, Y.-N. Liu, X. Zhou, C.-Z. Yuan, A.-W. Xu, *RSC Adv.* **2016**, *6*, 52937.
[30] H. Kim, J. Lee, H. Ahn, O. Kim, M. J. Park, *Nat. Commun.* **2015**, *6*, 7278.
[31] S. Hong, W. Chen, Y. Zhang, H. Q. Luo, M. Li, N. B. Li, *Corros. Sci.* **2013**, *66*, 308.
[32] C.-C. Höhne, C. Posern, U. Böhme, E. Kroke, *Chem. Eur. J.* **2018**, *24*, 13596.
[33] a) G. Zhang, J. Zhang, M. Zhang, X. Wang, *J. Mater. Chem.* **2012**, *22*, 8083; b) J. Hong, X. Xia, Y. Wang, R. Xu, *J. Mater. Chem.* **2012**, *22*, 15006.
[34] J. Zhang, J. Sun, K. Maeda, K. Domen, P. Liu, M. Antonietti, X. Fu, X. Wang, *Energy Environ. Sci.* **2011**, *4*, 675.
[35] M. W. Beukers, L. C. W. Chang, J. K. von Frijtag Drabbe Künzel, T. Mulder-Krieger, R. F. Spanjersberg, J. Brussee, A. P. IJzerman, *J. Med. Chem.* **2004**, *47*, 3707.
[36] M. P. Cava, M. I. Levinson, *Tetrahedron* **1985**, *41*, 5061.
[37] H. Rostkowska, L. Lapinski, A. Khvorostov, M. J. Nowak, *J. Phys. Chem. A* **2005**, *109*, 2160.
[38] R. C. Hirt, R. G. Schmitt, H. L. Strauss, J. G. Koren, *Chem. Zentralbl.* **1962**, *133*, 8203; alternative source: R. C. Hirt, R. G. Schmitt, H. L. Strauss, J. G. Koren, *J. Chem. Eng. Data* **1961**, *6*, 610.
[39] K. R. Henke, A. R. Hutchison, M. K. Krepps, S. Parkin, D. A. Atwood, *Inorg. Chem.* **2001**, *40*, 4443.
[40] C. E. Redemann, H. J. Lucas, *J. Am. Chem. Soc.* **1939**, *61*, 3420.
[41] a) M. Takimoto, *Nippon Kagaku Zasshi* **1964**, *85*, 159–168; b) G. Huyge-Tiprez, J. Nicole, *C. R. Seances Acad. Sci. Ser. C* **1977**, *284*, 913.
[42] F. Belaj, R. Tripolt, E. Nachbaur, *Monatsh. Chem.* **1990**, *121*, 99.
[43] Y. Ke, D. J. Collins, D. Sun, H.-C. Zhou, *Inorg. Chem.* **2006**, *45*, 1897.
[44] a) A. S. Jessiman, D. D. MacNicol, P. R. Mallinson, I. Vallance, *J. Chem. Soc. Chem. Commun.* **1990**, 1619; b) P. Bombicz, A. Kálmán, *Cryst. Growth Des.* **2008**, *8*, 2821; c) V. R. Thalladi, S. Brasselet, H.-C. Weiss, D. Bläser, A. K. Katz, H. L. Carrell, R. Boese, J. Zyss, A. Nangia, G. R. Desiraju, *J. Am. Chem. Soc.* **1998**, *120*, 2563.
[45] *X-RED and X-AREA*, Stoe & Cie, Darmstadt, Germany, **2009**.
[46] *X-Shape*, Stoe & Cie, Darmstadt, Germany, **2010**.
[47] G. M. Sheldrick, *Acta Crystallogr. Sect. A* **2008**, *64*, 112.
[48] G. M. Sheldrick, *Acta Crystallogr. C* **2015**, *71*, 3.
[49] W. L. F. Armarego, C. L. L. Chai, *Purification of laboratory chemicals*, Butterworth-Heinemann, Oxford, **2009**.
[50] M. J. Frisch, G. W. Trucks, H. B. Schlegel, G. E. Scuseria, M. A. Robb, J. R. Cheeseman, G. Scalmani, V. Barone, G. A. Petersson, H. Nakatsuji, X. Li, M. Caricato, A. V. Marenich, J. Bloino, B. G. Janesko, R. Gomperts, B. Mennucci, H. P. Hratchian, J. V. Ortiz, A. F. Izmaylov, J. L. Sonnenberg, D. Williams-Young, F. Ding, F. Lipparini, F. Egidi, J. Goings, B. Peng, A. Petrone, T. Henderson, D. Ranasinghe, V. G. Zakrzewski, J. Gao, N. Rega, G. Zheng, W. Liang, M. Hada, M. Ehara, K. Toyota, R. Fukuda, J. Hasegawa, M. Ishida, T. Nakajima, Y. Honda, O. Kitao, H. Nakai, T. Vreven, K. Throssell, Montgomery, Jr., J. A., J. E. Peralta, F. Ogliaro, M. J. Bearpark, J. J. Heyd, E. N. Brothers, K. N. Kudin, V. N. Staroverov, T. A. Keith, R. Kobayashi, J. Normand, K. Raghavachari, A. P. Rendell, J. C. Burant, S. S. Iyengar, J. Tomasi, M. Cossi, J. M. Millam, M. Klene, C. Adamo, R. Cammi, J. W. Ochterski, R. L. Martin, K. Morokuma, O. Farkas, J. B. Foresman, D. J. Fox, *Gaussian 16 Revision B.01*, Gaussian, Inc., Wallingford CT, **2016**.

[51] a) Y. Zhao, D. G. Truhlar, *Theor. Chem. Acc.* **2008**, *120*, 215; b) P. C. Hariharan, J. A. Pople, *Theor. Chim. Acta* **1973**, *28*, 213; c) M. M. Francl, W. J. Pietro, W. J. Hehre, J. S. Binkley, M. S. Gordon, D. J. DeFrees, J. A. Pople, *J. Chem. Phys.* **1982**, *77*, 3654.

[52] E. D. Glendening, J. K. Badenhoop, A. E. Reed, J. E. Carpenter, J. A. Bohmann, C. M. Morales, C. R. Landis, F. Weinhold, *NBO 6.0*, Theoretical Chemistry Institute, University of Wisconsin, **2013**.

Manuscript received: July 25, 2019
Accepted manuscript online: September 24, 2019
Version of record online: November 6, 2019

